

Effects of the V_2O_5 Additive on $ZnNb_2O_6$ Microwave Dielectrics

Sung-Hun Wee, Dong-Wan Kim, Sang-Im Yoo[†] and Kug Sun Hong

School of Materials Science and Engineering, Seoul National University, Seoul 151-742, Korea

(Received February 10, 2001, Accepted April 11, 2001)

ABSTRACT

We report the effects of the V_2O_5 additive on the sintering behavior and microwave dielectric properties of $ZnNb_2O_6$ ceramics. Densification temperatures of V_2O_5 -doped $ZnNb_2O_6$ samples are lowered to the range of 875–925°C because of the liquid phase sintering. Doped samples are composed of a $Zn(Nb,V)_2O_6$ solid solution and second phases. Up to 5 wt% V_2O_5 addition, $V_3Nb_{17}O_{50}$ is the only second phase, however, V_2O_5 also exists as the second phase for 10 wt% V_2O_5 addition. In comparison with reported values of undoped $ZnNb_2O_6$ ceramics, microwave properties of V_2O_5 -doped $ZnNb_2O_6$ samples are seriously degraded, which is confirmed to originate from the second phases. The optimum microwave properties ($Q \times f = 13,800$, $\epsilon_r = 23$, and $\tau_f = -66$ ppm/°C) are obtained from $ZnNb_2O_6$ with the addition of 5 wt% V_2O_5 sintered at 900°C.

Key words : $ZnNb_2O_6$, V_2O_5 , Microwave dielectric properties, Sintering, Densification

1. Introduction

Microwave dielectrics have been used as key components in mobile and satellite communications, including duplex filter, band pass filter, voltage controlled oscillator, dielectric resonator, and planar antenna¹⁾. Recent development in mobile communication, however, requires the miniaturization of microwave dielectrics to produce multi-layer or chip devices like a multi chip module (MCM). Particularly for the fabrication of MCM, low temperature co-fired ceramics (LTCC) are widely being studied²⁾ since if densification temperature is lowered below the melting point (960°C) of Ag, current expensive electrodes such as Pt, Pd, and Au can be replaced by less expensive Ag.

Maeda *et al.*³⁾ first reported on the microwave dielectric properties (quality factor, $Q \times f = 44,000$, dielectric constant, $\epsilon_r = 20$) of $ZnNb_2O_6$ ceramics for a sample sintered at 1200°C. More recently, Lee *et al.*⁴⁾ reported much improved microwave properties ($Q \times f = 83,700$ and $\epsilon_r = 25$) for a $ZnNb_2O_6$ sample sintered at 1150°C. They also reported that $ZnNb_2O_6$ exhibited the highest $Q \times f$ value among the MNb_2O_6 (M: Ca, Co, Mn, Ni, Zn) compounds which commonly have the columbite structure. Although microwave dielectric properties of $ZnNb_2O_6$ are quite excellent, the application of this material to MCM using the Ag electrode has been hindered because densification is possible at the temperature above 1150°C.

In general, a sintering aid has been employed to lower the densification temperature in ceramics, which is also the case for LTCC microwave dielectrics. Among various potential additives, V_2O_5 has been selected as the sintering aid for

$ZnNb_2O_6$ in the present study since it has been proved effective for lowering the densification temperature of other microwave dielectric ceramics⁵⁻⁸⁾. Unfortunately, it is also reported that microwave dielectric properties are seriously degraded with its addition although the origin for this degradation has been unclarified yet. In this study, we carefully investigated whether V_2O_5 would be also effective in lowering the densification temperature of $ZnNb_2O_6$ and how microwave dielectric properties of $ZnNb_2O_6$ would be affected by the V_2O_5 additive. A particular attention has been paid to identify the important factors governing microwave dielectric properties of V_2O_5 -doped $ZnNb_2O_6$.

2. Experimental

Precursors were ZnO, Nb_2O_5 , and V_2O_5 powders with high purity (>99.9%). $ZnNb_2O_6$ was first prepared with the following procedure. Precursors of ZnO and Nb_2O_5 were weighed and mixed with a dry ball-mill. The materials were pressed into pellets and calcined twice for 2 h at 1000°C with an intermediate grinding and pressing. Next, various amounts (3, 5, and 10 wt%) of V_2O_5 were added to as-calcined $ZnNb_2O_6$ powder. The powder mixture was ball-milled for 48 h in a polyethylene jar with zirconia balls using ethanol as a medium. The milled powders were dried, granulated with addition of 10 wt% PVA (poly vinyl alcohol) solutions, and pressed into pellets at 1.5 ton/cm². Pressed pellets were put into a muffle furnace, heated to various high temperatures (875–1000°C)-with a heating rate of 5°C/min to be held for 2 h, and finally furnace-cooled.

Thermal analyses were performed using differential thermal analysis (DTA). Shrinkage of the specimens was measured using a horizontal loading dilatometry with alumina

[†]Corresponding author : siyoo@plaza.snu.ac.kr

rams and boats at the heating rate of $5^\circ\text{C}/\text{min}$. Phase identification was performed using the powder x-ray diffraction (XRD). Sintered density was measured by Archimedes method. Microstructural analyses were performed by scanning electron microscopy (SEM). Compositional analyses were performed with energy dispersive x-ray spectroscopy (EDS) equipped to a transmission electron microscope (TEM).

Microwave dielectric properties of sintered samples were measured using a network analyzer (Model HP8720C) in the frequency range of 9-12 GHz. Relative dielectric constant (ϵ_r) was measured using the post resonator method⁹. The quality factor ($Q \times f$) was measured by the transmission cavity method using a Cu cavity and Teflon supports¹⁰ and the temperature coefficient of the resonant frequency (τ_f) was measured using invar cavity in the temperature range of 20 to 80°C ¹¹.

3. Results and Discussion

In order to identify the role of the V_2O_5 additive on the sintering behavior of $ZnNb_2O_6$, we first performed DTA analyses as shown in Fig. 1. In the case of V_2O_5 , the endothermic hump with the onset temperature of 671°C is attributed to its melting event since temperatures like 690°C ^{12,13} and 675°C ¹⁴ have been reported as the melting point of V_2O_5 in the literature. For the 10 wt% V_2O_5 -doped $ZnNb_2O_6$, the endothermic hump with the onset temperature of 653°C is attributed to the formation of a liquid phase by the chemical reaction between V_2O_5 and $ZnNb_2O_6$. Referring to the phase diagrams of V_2O_5 -ZnO binary¹³ and V_2O_5 - Nb_2O_5 binary¹⁴, V_2O_5 represents eutectic reactions with ZnO and Nb_2O_5 at the eutectic points of $627 \pm 10^\circ\text{C}$ and 648°C , respectively. As a result, the thermal event at 653°C is due to the liquid phase formation by a ternary eutectic reaction.

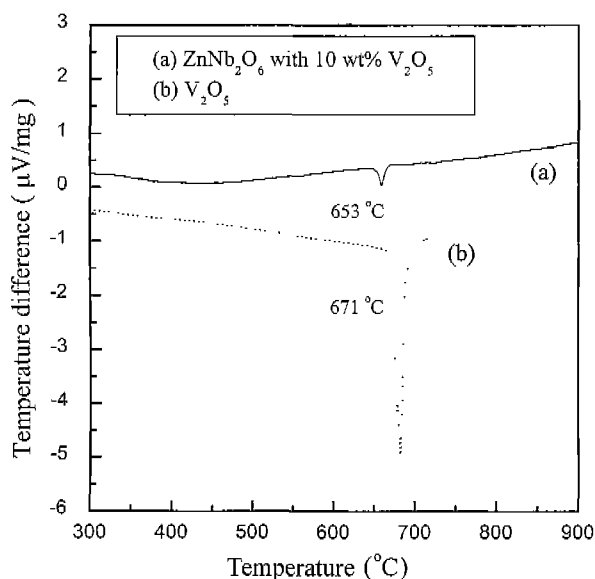


Fig. 1. DTA curves of (a) $ZnNb_2O_6$ with 10 wt% V_2O_5 additive and (b) V_2O_5 .

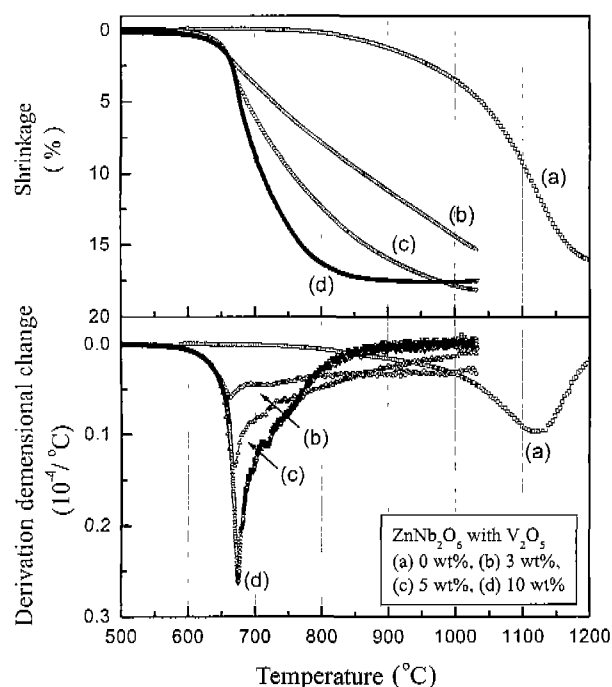


Fig. 2. Shrinkage and derivation dimensional change of $ZnNb_2O_6$ samples with the additives of (a) 0 wt% V_2O_5 , (b) 3 wt% V_2O_5 , (c) 5 wt% V_2O_5 , (d) 10 wt% V_2O_5 , respectively.

To further understand whether the above liquid phase formation in the V_2O_5 -doped $ZnNb_2O_6$ samples would actually lead to densification at the temperature above 653°C , shrinkage measurements were performed for the specimens of as-pressed pellets as shown in Fig. 2. While undoped $ZnNb_2O_6$ specimen exhibits the shrinkage onset at $\sim 800^\circ\text{C}$ and the maximum shrinkage variation within the temperature region of 1100 - 1150°C , V_2O_5 -doped $ZnNb_2O_6$ specimens commonly exhibit the shrinkage onset at $\sim 600^\circ\text{C}$ and the maximum shrinkage variation within the temperature region of 650 - 700°C . It is also shown that the shrinkage becomes larger with increasing the amount of the V_2O_5 additive below 950°C . Interestingly, the specimen with 10 wt% V_2O_5 additive does not show shrinkage at the temperature above 850°C , implying densification would occur below 900°C . These results suggest that the V_2O_5 additive would be very effective for the densification of $ZnNb_2O_6$ at relatively low firing temperatures by the liquid phase sintering.

Fig. 3 shows the XRD patterns of samples sintered for 2 h at 900°C . Small extra peaks, which are absent in the pure $ZnNb_2O_6$ sample in Fig. 4(a), are found for the V_2O_5 -doped samples in Fig. 4(b)-(d). With the aid of JCPDS (Joint Committee on Powder Diffraction Standards), we could figure out that these peaks are originated from two different second phases of $V_3Nb_{17}O_{50}$ and V_2O_5 . Up to 5 wt% V_2O_5 addition, only $V_3Nb_{17}O_{50}$ phase is observed. However, with 10 wt% V_2O_5 addition, V_2O_5 also appears as the second phase. In Fig. 3, it is also observed that the major peak positions of the V_2O_5 -doped $ZnNb_2O_6$ samples shift to higher 2θ in com-

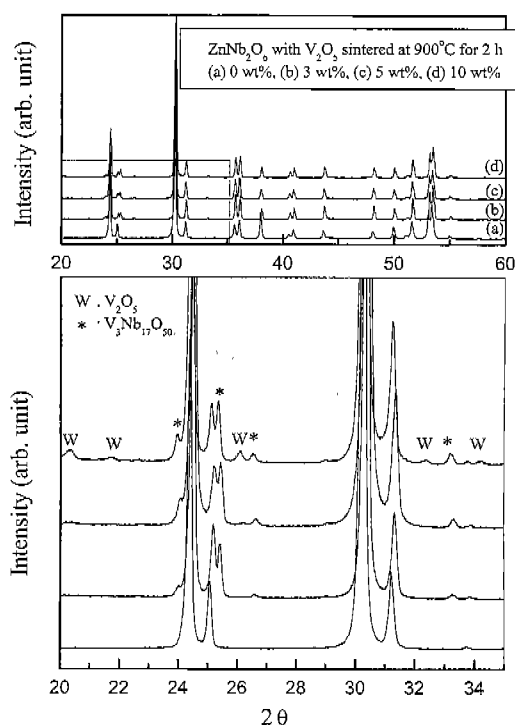


Fig. 3. XRD patterns of ZnNb_2O_6 samples with the additives of (a) 0 wt% V_2O_5 , (b) 3 wt% V_2O_5 , (c) 5 wt% V_2O_5 , (d) 10 wt% V_2O_5 . All samples were sintered at 900°C .

parison with pure ZnNb_2O_6 . To identify the origin of this peak shift, the composition of the matrix phase of V_2O_5 -doped specimen was analyzed with TEM-EDS. The EDS analysis result exhibited the existence of 4 mol% V component in addition to Zn, Nb, and O, implying that ZnNb_2O_6 has a limited solubility of V. If we consider the ionic size of these components, V^{5+} ions most probably occupy the Nb^{5+} site to form the $\text{Zn}(\text{Nb}_x\text{V}_{1-x})_2\text{O}_6$ solid solutions, which might cause the above XRD peak shifts.

In order to identify the formation procedure of second phases, we have also performed XRD analyses for 10 wt% V_2O_5 -doped ZnNb_2O_6 samples, rapidly quenched from various high temperatures in air. The results are shown in Fig. 4. Below the liquid formation temperature of 653°C , the $\text{V}_4\text{Nb}_{18}\text{O}_{55}$ phase is first formed as the major second phase through a solid state reaction between V_2O_5 and ZnNb_2O_6 . In the temperature range between 675°C and 750°C , the $\text{V}_3\text{Nb}_{17}\text{O}_{50}$ phase also appears and coexists with the $\text{V}_4\text{Nb}_{18}\text{O}_{55}$ phase. Between 700°C and 750°C , the $\text{V}_4\text{Nb}_{18}\text{O}_{55}$ phase completely disappears and the $\text{V}_3\text{Nb}_{17}\text{O}_{50}$ phase still exists. The $\text{V}_3\text{Nb}_{17}\text{O}_{50}$ phase is stable above 750°C and hence it is detected as the second phase of V_2O_5 -doped ZnNb_2O_6 samples sintered at the temperature range of 875 – 925°C . In the case of the V_2O_5 second phase, it is detected only for 10 wt% V_2O_5 addition as previously mentioned. While the peaks due to the V_2O_5 phase exist in the whole temperature range, it is obvious that the XRD peaks become very broad at the firing temperature above 675°C as shown in Fig. 4. Since the melt-

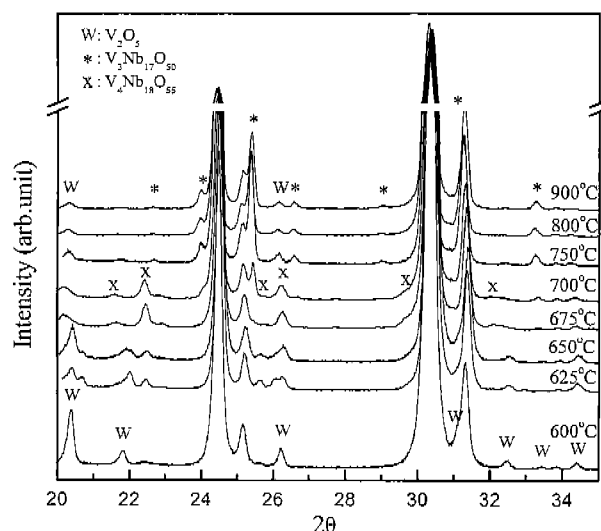


Fig. 4. XRD patterns of 10 wt% V_2O_5 -doped ZnNb_2O_6 samples quenched from various high temperatures in air.

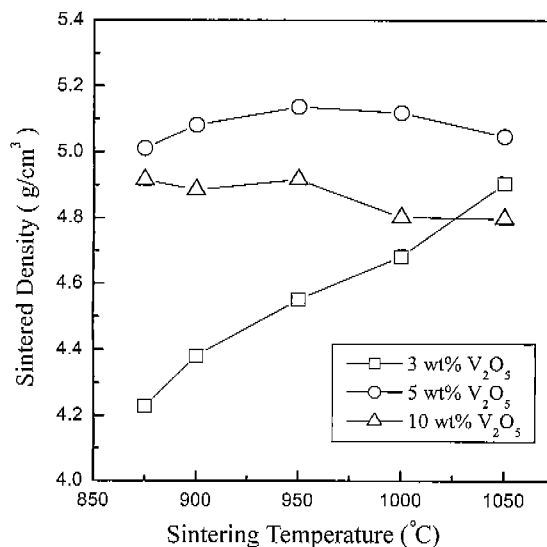


Fig. 5. Sintered density of V_2O_5 -doped ZnNb_2O_6 samples as a function of the sintering temperature.

ing point of V_2O_5 is 671°C , the V_2O_5 phase detected above 675°C is surely a byproduct solidified from the liquid phase during air-quenching.

Fig. 5 represents the sintered density of V_2O_5 -doped ZnNb_2O_6 samples as a function of the sintering temperature. While sintered densities of samples with 3 wt% V_2O_5 monotonously increase with increasing the sintering temperature, those of samples with V_2O_5 more than 5 wt% are not altered significantly above 900°C . Here, it should be noted that at least 1150°C is required for the densification of pure ZnNb_2O_6 . Since the theoretical density of pure ZnNb_2O_6 is 5.645 g/cm^3 , the highest sintered density of 5.137 g/cm^3 obtained from the sample of 5 wt% V_2O_5 -doped ZnNb_2O_6 sintered at 950°C corresponds to only 91% relative density on the basis of pure ZnNb_2O_6 . Thus, relatively low sintered

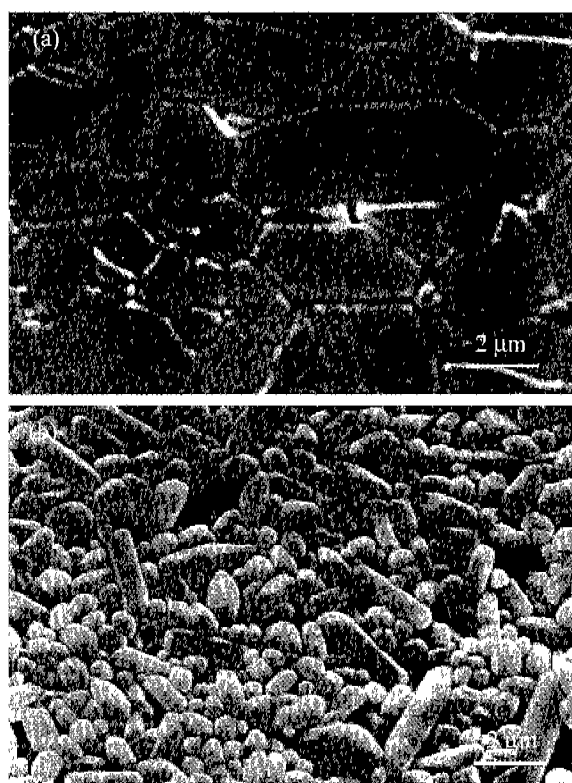


Fig. 6. SEM Micrographs of (a) pure $ZnNb_2O_6$ sintered at 1150°C and (b) 10 wt% V_2O_5 -doped $ZnNb_2O_6$ sintered at 900°C .

densities of V_2O_5 -doped samples are ascribed to the existence of second phases since theoretical densities of $V_3Nb_{17}O_{50}$ and V_2O_5 second phases are 3.46 g/cm^3 and 4.46 g/cm^3 , respectively.

SEM micrographs of samples are shown in Fig. 6. To obtain a clear grain boundary, both pure and 10 wt% V_2O_5 -doped $ZnNb_2O_6$ samples were thermally etched at 1000°C and 700°C for 1 h, respectively. In comparison with pure $ZnNb_2O_6$ in Fig. 6(a), doped sample in Fig. 6(b) exhibits much smaller grain size although grain shapes are not much different. Although not presented, SEM micrographs of samples with 3 and 5 wt% V_2O_5 and sintered at 900°C are very similar to Fig. 6(b). From Fig. 6(b), it is clear that the sample sintered at 900°C is very dense, which also supports that low sintered densities of doped samples in Fig. 5 are

attributed to the inclusion of the second phases.

Microwave dielectric properties of V_2O_5 -doped $ZnNb_2O_6$ samples are represented in Table 1. For a comparison, reported data of pure $ZnNb_2O_6$ samples are also listed in the table. Unfortunately, it is obvious that the addition of V_2O_5 to $ZnNb_2O_6$ greatly decreases the quality factor, $Q \times f$. The dielectric constant, ϵ_r , also becomes relatively smaller and the temperature coefficient of the resonant frequency, τ_f , values becomes more negative. Similar results are also found for other microwave dielectrics with the V_2O_5 additive⁵⁻⁸⁾ although the origin for this degradation was unclarified in these reports.

For V_2O_5 -doped $ZnNb_2O_6$ samples, we have identified important factors leading to a serious degradation of their microwave dielectric properties in Table 1. Possible origins of this degradation surely ascribe to the formation of $Zn(Nb,V)_2O_6$ solid solution and/or the second phases. At first, we have tried to identify the effect of the $Zn(Nb,V)_2O_6$ matrix phase on the microwave properties. For this purpose, a pure $Zn(Nb_{0.96}V_{0.04})_2O_6$ sample without any second phases was prepared independently. We selected this composition on the basis of the TEM-EDS analysis result previously described. Interestingly, a highly dense sample of this composition could be obtained at the sintering temperature of 900°C in air. Microwave dielectric properties of this sample are listed in Table 1. Therefore, such an abrupt decrease of the quality factor, $Q \times f$ shown in Table 1 is unattributable to the formation of $Zn(Nb,V)_2O_6$ solid solution. Here, it is noteworthy that a small amount of the V component for the substitution of the Nb site is very effective for the low temperature sintering without such a serious degradation of microwave properties. Detailed study for this system is in progress.

As the $Zn(Nb,V)_2O_6$ matrix phase is not the origin of the property degradation, it is thus natural to find the origin from the second phases. The $V_3Nb_{17}O_{50}$ phase is the major second phase in the $ZnNb_2O_6$ samples of 3 and 5 wt% V_2O_5 additives (see Fig. 3). Since these samples commonly exhibit much depressed quality factors compared to pure $ZnNb_2O_6$ samples (Table 1), it is suggested that the degradation of the quality factor, $Q \times f$ is primarily attributed to the $V_3Nb_{17}O_{50}$ second phase. To ensure this point, a pure $V_3Nb_{17}O_{50}$ sample was prepared at the sintering temperature of 1050°C , independently. Below this temperature, densifica-

Table 1. Microwave Dielectric Properties of Pure and V_2O_5 -doped $ZnNb_2O_6$ Samples

Compositions	Sintering Conditions	$Q \times f$	ϵ_r	τ_f (ppm/ $^\circ\text{C}$)
$ZnNb_2O_6$ (Maeda <i>et al.</i>) ⁹⁾	1200°C , 5 h	44,000	20	x
$ZnNb_2O_6$ (Lee <i>et al.</i>) ⁴⁾	1150°C , 2 h	83,700	22	-56
$ZnNb_2O_6$ + 3 wt% V_2O_5	950°C , 2 h	13,900	18	-80
$ZnNb_2O_6$ + 5 wt% V_2O_5	900°C , 2 h	13,800	23	-66
$ZnNb_2O_6$ + 10 wt% V_2O_5	900°C , 2 h	10,300	22	-83
$Zn(Nb_{0.96}V_{0.04})_2O_6$	900°C , 2 h	47,000	22	-64

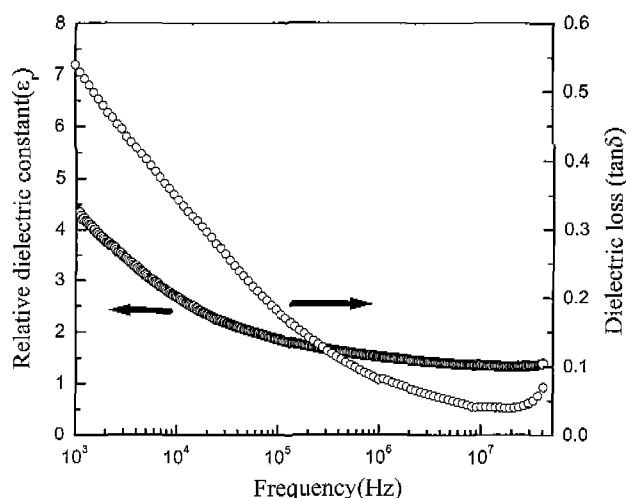


Fig. 7. Dielectric properties of a pure $V_3Nb_{17}O_{50}$ sample sintered at 1050°C .

tion was not achieved. The microwave properties of this sample were unmeasurable in the microwave frequency region. Thus, we measured dielectric properties in the relatively low frequency region (1 kHz - 40 MHz), as shown in Fig. 7. Relatively high dielectric loss and very low dielectric constant even in this frequency region are observed from this figure. Therefore, a serious degradation of dielectric properties is expected to occur in the microwave region. Although not measured, the V_2O_5 second phase existing in the 10 wt% V_2O_5 -doped sample is considered to behave like the $V_3Nb_{17}O_{50}$ second phase. Consequently, we could figure out that the abrupt degradation of microwave properties for V_2O_5 -doped samples are surely due to the presence of the second phases possessing very poor microwave properties.

In summary, with the V_2O_5 additive, sintering temperature of $ZnNb_2O_6$ could be lowered from 1150°C to the range of $875\text{--}925^\circ\text{C}$. The densification at such a low firing temperature was enabled by the liquid phase sintering, where the liquid phase was formed from the reaction between $ZnNb_2O_6$ and V_2O_5 . The addition of V_2O_5 to $ZnNb_2O_6$ resulted in the formation of the $Zn(Nb,V)_2O_6$ solid solution matrix and the second phases. Up to 5 wt% V_2O_5 addition, $V_3Nb_{17}O_{50}$ was the only second phase while V_2O_5 phase was found as well for 10 wt% V_2O_5 addition. In comparison with undoped $ZnNb_2O_6$, V_2O_5 -doped $ZnNb_2O_6$ exhibited much degraded microwave dielectric properties. This degradation is attributed to the second phases of $V_3Nb_{17}O_{50}$ and V_2O_5 , exhibiting relatively high dielectric loss and very low dielectric constant even in the frequency region of 1 kHz - 40 MHz. The optimum microwave dielectric property of $Q \times f = 13,800$, $\epsilon_r = 23$, $\tau_f = -66 \text{ ppm}/^\circ\text{C}$ was achieved from the 5 wt% V_2O_5 -doped sample sintered at 900°C for 2 h.

4. Conclusion

With the V_2O_5 addition to $ZnNb_2O_6$ microwave ceramics, while densification temperature can be lowered below the

melting point of Ag because of the liquid phase sintering, microwave dielectric properties are seriously degraded in comparison with pure $ZnNb_2O_6$. This serious degradation is caused by the inclusion of the second phases such as $V_3Nb_{17}O_{50}$ and V_2O_5 . Particularly, the formation of the $V_3Nb_{17}O_{50}$ phase is unavoidable for the present system. One way to detour this problem seems to form a $Zn(Nb,V)_2O_6$ -type solid solution by substituting the Nb site with the V component since densification occurred at the temperature like 900°C and its microwave properties are not much degraded, which however requires further study.

Acknowledgements

This work is partially supported by the Korean Science and Engineering Foundation (KOSEF) through the Center for Strongly Correlated Materials Research (CSCMR) (2000).

REFERENCES

1. W. Wersing, *Electronic Ceramics*, Ed. B. C. H. Steele, Elsevier Applied Science, 67-119 (1991).
2. T. K. Gupta and J. H. Jean, "Principles of the Development of a Silica Dielectric for Microelectronics," *J. Mater. Res.*, **11**(1), 243-263 (1996).
3. M. Maeda, T. Yamamura and T. Ikeda, "Dielectric Characteristics of Several Complex Oxide Ceramics at Microwave Frequencies," *Jpn. J. Appl. Phys.*, **26**, 76-79 (1987).
4. H.-J. Lee, "Dielectric Properties of MNb_2O_6 Compounds (where $M=\text{Ca, Mn, Co, Ni, or Zn}$)," *Mater. Res. Bull.*, **32**(7), 847-855 (1997).
5. H. Yamamoto, A. Koga, S. Shibagaki and N. Ichinose, "Low Temperature Firing of $\text{MaTiO}_3\text{-CaTiO}_3$ Microwave Dielectric Ceramics Modified with B_2O_3 and V_2O_5 ," *J. Ceram. Soc. Jpn.*, **106**(3), 339-343 (1998).
6. H. Kagata, T. Inoue, J. Kato and I. Kameyama "Low-fire Bismuth-based Dielectric Ceramics for Microwave Use," *Jpn. J. Appl. Phys.*, **31**, 3152-3155 (1992).
7. W.-C. Tzou, C.-F. Yang, Y.-C. Chen and P.-S. Cheng, "Improvements in the Sintering and Microwave Properties of BiNbO_4 Microwave Ceramics by V_2O_5 Addition," *J. Euro. Ceram. Soc.*, **20**, 991-996 (2000).
8. C.-L. Huang, M.-H. Weng and G.-M. Shan, "Effect of V_2O_5 and CuO Additives on Sintering Behavior and Microwave Dielectric Properties of BiNbO_4 Ceramics," *J. Mater. Sci.*, **35**, 5443-5447 (2000).
9. B. W. Hakki and P. D. Coleman, "A Dielectric Resonator Method of Measuring Inductive Capacities in the Millimeter Range," *IRE Trans. Microwave Theory & Technol.*, **8**, 402-410 (1960).
10. D. Kaifez and P. Guillion, *Dielectric Resonator*, Artech House, Norwood, MA, 327-376 (1986).
11. T. Nishikawa, K. Wakino, H. Tamura, H. Tanaka and Y. Ishikawa, "Precise Measurement Method For Temperature Coefficient of Microwave Dielectric Resonator Material," *IEEE MTT-S Digest*, **3**, 277-280 (1987).
12. *Merck Index* (Twelfth edition), 10054.

13. E. Pollert, "A Contribution to the Phase Diagram of the System $ZnO-V_2O_5$," *Silikaty (Prague)*, **17**(2), 103-108 (1973).
14. J. L. Waring and R. S. Roth, "Phase Equilibria in the System Vanadium Oxide-niobium Oxide," *J. Res. Natl. Bur. Stand. A*, **69**(2), 119-129 (1965).